British Journal of Pharmacology (2000) 130, 669–677

www.nature.com/bjp

High affinity interaction of mibefradil with voltage-gated calcium and sodium channels

[1]Philipp Eller, [1]Stanislav Berjukov, [1]Siegmund Wanner, [1]Irene Huber, [1]Steffen Hering, [1]Hans-Günther Knaus, [2]Geza Toth, [3]S. David Kimball & *,[1]Jörg Striessnig

[1]Institut für Biochemische Pharmakologie, Peter-Mayrstr. 1, A-6020 Innsbruck, Austria; [2]Biological Research Center, Institute of Biochemistry, H-6726 Szeged, Hungary and [3]Bristol-Myers Squibb Pharmaceutical Company, P.O. Box 4000, Princeton, New Jersey, NJ 08543-4000, U.S.A.

1 Mibefradil is a novel Ca^{2+} antagonist which blocks both high-voltage activated and low voltage-activated Ca^{2+} channels. Although L-type Ca^{2+} channel block was demonstrated in functional experiments its molecular interaction with the channel has not yet been studied. We therefore investigated the binding of [^{3}H]-mibefradil and a series of mibefradil analogues to L-type Ca^{2+} channels in different tissues.

2 [^{3}H]-Mibefradil labelled a single class of high affinity sites on skeletal muscle L-type Ca^{2+} channels (K_D of 2.5 ± 0.4 nM, $B_{max} = 56.4 \pm 2.3$ pmol mg^{-1} of protein).

3 Mibefradil (and a series of analogues) partially inhibited (+)-[^{3}H]-isradipine binding to skeletal muscle membranes but stimulated binding to brain L-type Ca^{2+} channels and α1C-subunits expressed in tsA201 cells indicating a tissue-specific, non-competitive interaction between the dihydropyridine and mibefradil binding domain.

4 [^{3}H]-Mibefradil also labelled a heterogenous population of high affinity sites in rabbit brain which was inhibited by a series of nonspecific Ca^{2+} and Na^+-channel blockers.

5 Mibefradil and its analogue RO40-6040 had high affinity for neuronal voltage-gated Na^+-channels as confirmed in binding (apparent K_i values of 17 and 1.0 nM, respectively) and functional experiments (40% use-dependent inhibition of Na^+-channel current by 1 μM mibefradil in GH3 cells).

6 Our data demonstrate that mibefradil binds to voltage-gated L-type Ca^{2+} channels with very high affinity and is also a potent blocker of voltage-gated neuronal Na^+-channels. More lipophilic mibefradil analogues may possess neuroprotective properties like other nonselective Ca^{2+}-/Na^+-channel blockers.

British Journal of Pharmacology (2000) **130,** 669–677

Keywords: Ca^{2+} channel blockers; sodium channel blockers; mibefradil

Abbreviations: BTZ, benzothiazepine; DHP, dihydropyridine; K_D, dissociation constant; PAA, phenylalkylamine

Introduction

The benzimidazolyl-substituted tetraline derivative mibefradil is a novel Ca^{2+} channel blocker with several interesting pharmacological properties. It blocks high-voltage-activated L-type Ca^{2+} channels in the cardiovascular system resulting in antihypertensive activity and slowing of heart rate without decreasing cardiac contractility (Clozel *et al*., 1997). Although mibefradil was withdrawn from the market due to pharmacokinetic interactions it remains an interesting pharmacological probe to investigate the contribution of individual ion channel subtypes for cardiovascular functions. In vascular and atrial myocytes it preferentially blocks low voltage-activated T-type Ca^{2+} channels suggesting that part of the bradycardic and vasodilating properties are mediated by block of these channels (Bezprozvanny & Tsien, 1995; Clozel *et al*., 1997). Heterologous expression of cloned Ca^{2+} channel α1 subunits confirmed block of both high (α1A, α1B, α1C, α1E; Bezprozvanny & Tsien, 1995) and low voltage-activated (α1G, α1H; Cribbs *et al*., 1998) Ca^{2+} channels by low micromolar concentrations of mibefradil. Block of L- (α1C) and non-L-type Ca^{2+} channels (α1A, α1B, α1E) occurred with similar IC_{50} values. It is therefore tempting to speculate that, if high affinity binding of tritiated mibefradil to L-type Ca^{2+} channels can be demonstrated, this radioligand should also be suitable for the reversible labelling of non-L-type Ca^{2+} channel complexes as well.

So far the binding of mibefradil to L-type Ca^{2+} channels has not been quantified in much detail. In preliminary studies the affinity of mibefradil for cardiac and smooth muscle channels was derived from its potency to displace (−)-[^{3}H]-devapamil from the phenylalkylamine (PAA) binding domain of the channel. IC_{50} estimates varied between 13 nM (Rutledge & Triggle, 1995) and 39 nM (Osterrieder & Holck, 1989). Direct labelling studies with [^{3}H]-mibefradil were hampered by the presence of low affinity sites (Ratner *et al*., 1996). Mibefradil failed to modulate (+)-[^{3}H]-isradipine binding to cardiac membranes and to polarized and depolarized cardiomyocytes (Rutledge & Triggle, 1995). This suggests that it binds to a site not coupled to the dihydropyridine (DHP) binding domain.

In order to establish the usefulness of [^{3}H]-mibefradil as a biochemical probe for voltage gated Ca^{2+} channels, we determined its binding properties in different excitable tissues using tritiated mibefradil and a series of unlabelled mibefradil analogues. We provide evidence that mibefradil labels a site on skeletal muscle and brain L-type Ca^{2+} channels which is tightly coupled to the DHP domain by a non-competitive binding mechanism. In addition, we found that mibefradil and

*Author for correspondence; E-mail: joerg.striessnig@uibk.ac.at

its analogues also display high affinity for neuronal voltage-gated Na^+-channels and potently block Na^+-currents in GH3 cells.

Methods

Materials

(+)-[^{3}H]-isradipine (≈79 Ci mmol^{-1}) was purchased from New England Nuclear (Vienna, Austria), (−)-[^{3}H]-devapamil (≈85 Ci mmol^{-1}) from Amersham (Vienna, Austria). [^{3}H]-SQ32133 (85 Ci mmol^{-1}) was synthesized by radioactive methylation of the corresponding phenol precursor. [^{3}H]-mibefradil (≈11.47 Ci mmol^{-1}) and [^{3}H]-WIN17317-3 (≈28.2 Ci mmol^{-1}) were provided by Hoffmann-La Roche (Basel, Switzerland) and by Merck (Rahway, NY, U.S.A.), respectively. Chemicals were obtained from the following sources: flunarizine, bovine serum albumin, phenylmethylsulphonyl fluoride and polyethylenimine from Sigma (Vienna, Austria), the stereoisomeres of verapamil, gallopamil and devapamil from Knoll (Ludwigshafen, Germany), the stereoisomeres of isradipine from Sandoz (Basel, Switzerland), fluspirilene and pimozide from Janssen (Beerse, Belgium), niguldipine from BYK Gulden (Konstanz, Germany), and diltiazem from Gödecke (Freiburg, Germany). Mibefradil (RO40-5967) and the mibefradil analogues (RO18-5881, RO19-6945, RO19-8287, RO19-8531, RO19-9495, RO40-0293, RO40-0713, RO40-6040, RO40-6088) (for chemical structures see Figure 1) were generously provided by Hoffmann-La Roche (Basel, Switzerland).

Membrane preparations and radioligand binding studies

Partially purified t-tubule membranes from rabbit skeletal muscle, rabbit cardiac membranes (Glossmann & Ferry, 1985), guinea-pig synaptic plasma membranes (Feigenbaum *et al*., 1988) and from transfected tsA201 cells were prepared as described and stored in liquid nitrogen until use. TsA201 cells were transfected with cDNA from α1C (Mitterdorfer *et al*., 1995) together with β1a and α2-δ (Mitterdorfer *et al*., 1995) (all cDNAs in plasmid pcDNA3) using the Ca^{2+} phosphate precipitation method. Membrane protein concentrations were determined according to Lowry (Lowry *et al*., 1951) with bovine serum albumin as a standard.

[^{3}H]-mibefradil equilibrium binding assay Binding assays were carried out at 25°C in 50 mM Tris-HCl, pH 7.4, 0.1 mM phenylmethylsulphonyl fluoride, 0.2 mg ml^{-1} bovine serum albumin (0.5–1 ml final assay volume). Nonspecific binding was defined in the presence of 1 μM mibefradil. Incubation lasted for 60–120 min. Bound ligand was determined by filtration of the assay mixture over GF/C Whatman filters pretreated with 0.25% (v v^{-1}) polyethyleneimine for about 30 min (Glossmann & Ferry, 1985). Filters were washed five times with ice-cold buffer (50 mM Tris-HCl, pH 7.4, 150 mM NaCl) and then counted for radioactivity by liquid scintillation counting. All drug solutions were prepared as 10 mM drug

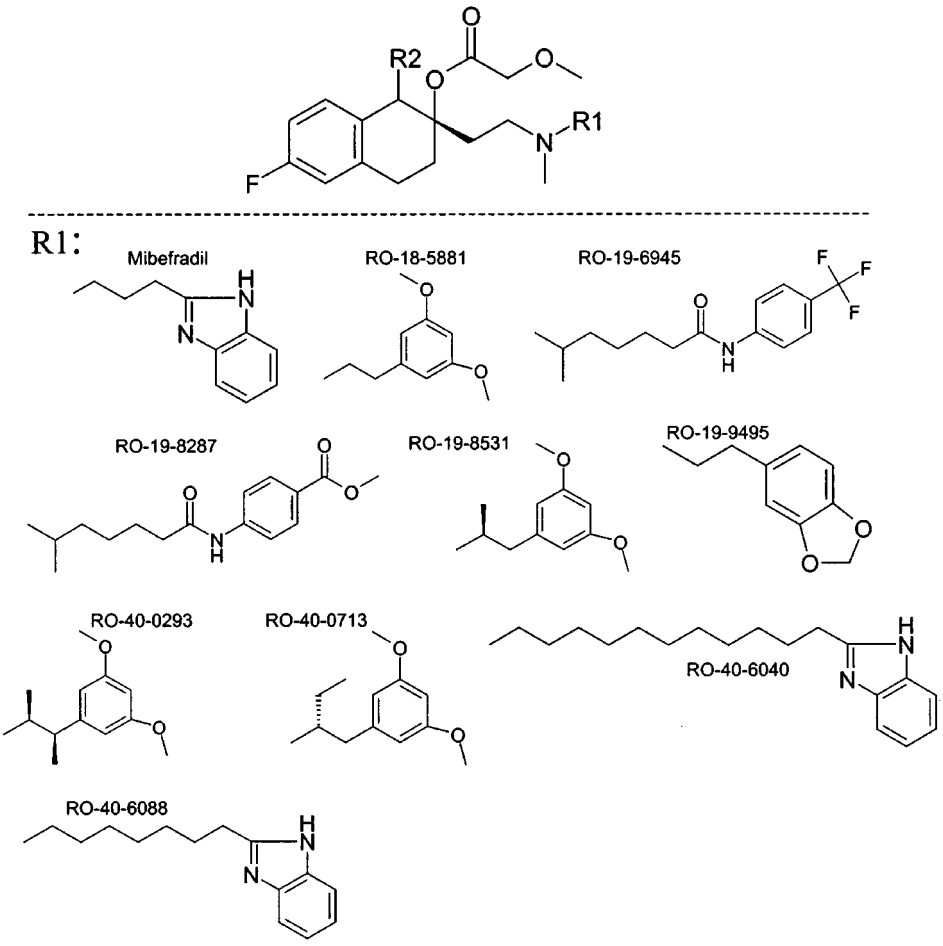

Figure 1 Chemical structure of mibefradil and mibefradil analogues. For stereochemistry of R2 see Table 1. R2 is isopropyl in all compounds. Note that RO-40-6088 contains a methoxyacetate group on the tetrahydronaphtyl ring instead of a methoxy group.

stock solutions in DMSO and stored at −25°C. The final DMSO concentration in the incubation mixture was ⩽1% (v v^{-1}) and did not affect radioligand binding. All experiments were done in duplicate.

(−)-[^{3}H]-devapamil, (+)-[^{3}H]-isradipine, [^{3}H]-SQ32133 and [^{3}H]-WIN17317-3 binding assays were performed as previously described (Kraus *et al*., 1998b; Prinz & Striessnig, 1993; Wanner *et al*., 1999). Nonspecific binding was defined by the presence of 1 μM (±)-isradipine, 3 μM (±)-devapamil, 10 μM (+)-cis-diltiazem and 1 μM WIN17317-3, respectively. Protein and radioligand concentrations are given in the figure legends.

To determine dissociation rate constants, radioligand and membranes were incubated until equilibrium was reached. The association reaction was blocked by an excess of unlabelled ligand or by 40 fold dilution of the assay mixture with assay buffer followed by filtration at the indicated times. Dissociation rate constants were determined as the slope of the regression line from a plot of ln (fractional binding) *versus* time. Association (k_{+1}) and dissociation (k_{-1}) rate constants were also calculated from association experiments by fitting the data to the differential equations describing a bimolecular reversible binding reaction using the software package SCIENTIST^R (MicroMath Inc.). The dissociation constants (K_D) and the maximal density of binding sites (B_{max}) were obtained by linear regression analysis after Scatchard transformation of the equilibrium saturation binding data.

Electrophysiological recordings

Inward Na^+ currents (I_{Na}) in GH3-cells (ATCC CCL82.1) were measured with the whole-cell configuration of the patch clamp technique (Hamill *et al*., 1981). Recordings were carried out at room temperature in an extracellular bath solution containing (mM) NaCl 140, $CaCl_2$ 1.8, $MgCl_2$ 2, 4-aminopyridine 5, tetraethylammonium chloride 5, HEPES 10 and glucose 10 (adjusted to pH 7.4 with NaOH). Data analysis and acquisition was performed by using the pClamp software package (version 6.0, Axon Instruments). The recording chamber (150 μl total volume) was continuously perfused at a flow rate of 1 ml min^{-1} with control and drug-containing solutions. I_{Na} was recorded after depolarization from a holding potential of −80 mV to a test potential of +5 mV. Initial 'tonic' block (resting state-dependent block) was defined as peak I_{Na} inhibition during the first pulse 2 min after drug application as compared with I_{Na} in the absence of drug. 'Use (frequency-)dependent' block of I_{Na} was measured during trains of 5 or 50 ms test pulses (3 Hz) applied from −80 mV to a test potential +5 mV after a 2-min equilibrium period in the drug-containing solution. Use-dependent block was expressed as the per cent decrease of peak I_{Na} during the last pulse of the train as compared with I_{Na} during the first pulse.

Data analysis

Nonlinear least square fitting and statistical calculations were performed using ORIGIN 5.0. Data are given as means± s.e.mean for the indicated number of experiments.

Results

High affinity binding of [^{3}H]-mibefradil to L-type Ca^{2+} channels in skeletal muscle

The basic binding properties of [^{3}H]-mibefradil (11.5 Ci $mmol^{-1}$) for L-type Ca^{2+} channels were determined in partially purified rabbit skeletal muscle transverse tubule membranes. After incubation for 60 min a saturable binding component was detected which increased linearly with membrane protein concentrations up to about 0.04 mg ml^{-1} (Figure 2A). Saturation analysis revealed a K_D of 2.5±0.4 nM and a B_{max} of 56.4±2.3 pmol mg^{-1} (n=8). Scatchard transformation of the saturation data was linear indicating labelling of a homogenous class of sites (Figure 2B, inset). The B_{max} was 2.6 fold higher than the B_{max} determined in parallel experiments for the DHP (+)-[^{3}H]-isradipine (21.8±0.6 pmol mg^{-1}, n=3) in the same membrane preparations. The high affinity was confirmed in kinetic experiments (Figure 2C). Mibefradil exhibited slow binding kinetics, with association and dissociation rate constants of 0.0104±0.0019 nM^{-1} min^{-1} (n=4) and 0.0226±0.0024 min^{-1} (n=7), respectively, yielding a kinetically derived K_D (k_{-1}/k_{+1}) of 2.2 nM. Dissociation was monophasic confirming the absence of site heterogeneity and increased with the concentration of cold ligand (Figure 2C). This ligand-induced accelerated dissociation has been described before for other cationic amphiphilic Ca^{2+} antagonists (Prinz & Striessnig, 1993).

[^{3}H]-Mibefradil binding was modulated by other chemical classes of Ca^{2+} antagonists. As shown in Figure 2D the enantiomers of the phenylakylamines verapamil, devapamil and gallopamil caused complete inhibition with IC_{50} values almost identical to those obtained after competitive displacement of (−)-[^{3}H]-devapamil from the PAA binding domain. The following IC_{50} values (and apparant Hill-slopes, n_H) for [^{3}H]-mibefradil inhibition were obtained by fitting the data of three independent experiments to the general-dose response equation: (−)-verapamil: 98±2.5 nM (0.93±0.05); (+)-verapamil: 66±6.3 nM (0.76±0.03); (−)-gallopamil: 25.3±0.8 (0.86±0.02); (+)-gallopamil: 122±20 nM (0.88±0.03); (−)-devapamil: 8.65±0.22 nM (0.89±0.02); (+)-devapamil: 35.5±5.3 nM (1.01±0.03). Almost identical binding parameters were obtained for (−)-[^{3}H]-devapamil labelled channels in parallel experiments (range, n=2): (−)-verapamil: 50–51 nM (0.83–0.88); (+) verapamil: 43–45 nM (0.96–1.00); (−)-gallopamil: 12–13 nM (0.99–1.08); (+)-gallopamil: 71–94 nM (0.85–1.20); (−)-devapamil: 2.9–5.7 nM (0.97–1.07); (+)-devapamil: 21–28 nM (1.2–1.5) (see also Goll *et al*., 1984a,b).

(−)-Isradipine also completely inhibited [^{3}H]-mibefradil binding, whereas (+)-isradipine was a partial inhibitor (Figure 3A).

As expected for L-type Ca^{2+} channels, [^{3}H]-mibefradil binding was also inhibited by divalent cations but not by Na^+ (Figure 3B) in a concentration range previously described for other Ca^{2+} channel ligands (Glossman *et al*., 1983; Goll *et al*., 1984b).

A series of mibefradil analogues with substituents of different length on the methylaminoethyl nitrogen revealed that replacement of the 3-(2-benzimidazoyl) propyl group by other substitutents (Table 1), or increase of its distance from the methylaminoethyl nitrogen (RO40-6040, RO40-6088) or introduction of one (RO19-8531) or two methyl groups (RO40-293) in this side chain was well tolerated. Replacement by a dimethoxyphenylethyl group (compound RO18-5881) even increased affinity (Table 1).

Figure 4A and Table 1 illustrate that unlabeled mibefradil also modulated the binding of Ca^{2+} antagonists to the DHP, PAA and benzothiazepine binding domain specifically labelled with (+)-[^{3}H]-isradipine, (−)-[^{3}H]-devapamil and [^{3}H]-SQ32,133 (Hering *et al*., 1993), respectively. Mibefradil was a partial inhibitor of (+)-[^{3}H]-isradipine binding. This inhibitory effect was converted to a stimulatory effect after side-chain

replacement with a dimethoxyphenylisopropyl group (RO19-8531, Figure 4A). Stimulation was critically dependent on the presence of a single methyl substituent on the ethyl linker (RO18-5881, complete inhibition; RO19-8531, stimulation;

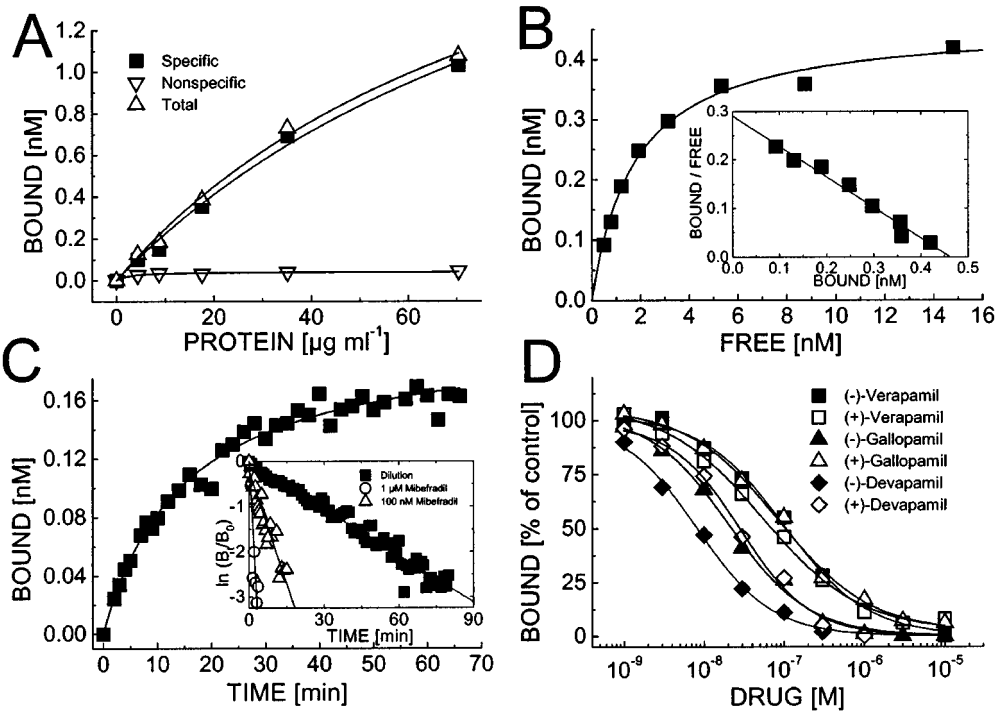

Figure 2 [^{3}H]-Mibefradil binding to partially purified rabbit skeletal muscle transverse tubule membranes. (A) Protein dependent binding: radioligand concentration was 2.9 nM. (B) Saturation analysis: Increasing concentrations of radioligand were incubated with 8.8 μg ml^{-1} of membrane protein for 60 min at 25°C before specific binding was determined. The following binding parameters were obtained after Scatchard transformation (inset) by linear regression analysis: r = 0.98, K_D = 1.6 nM; B_{max} = 52.4 pmol mg^{-1} membrane protein. (C) Association kinetics. 2.3 nM [^{3}H]-mibefradil was incubated with 4.4 μg ml^{-1} membrane protein for the indicated times before specific binding was measured. The following binding parameters resulted from non-linear curve fitting to a bimolecular binding reaction as described in the Methods section: k_{+1} = 0.0087 min^{-1} nM^{-1}; k_{-1} = 0.0327 min^{-1}; calculated K_D = 3.8 nM. Dissociation kinetics (inset). After specific binding equilibrium was reached (B_0) dissociation was initiated by 40 fold dilution or by addition of 100 nM or 1 μM mibefradil. The following dissociation rate constants were calculated by linear regression from semilogarithmic plots: k_{-1} = 0.034 min^{-1} (■); k_{-1} = 0.166 min^{-1} (△); k_{-1} = 0.99 min^{-1} (○). (D) Inhibition of [^{3}H]-mibefradil by phenylalkylamines; membrane protein concentration = 4.4 μg ml^{-1}; radioligand concentration = 1–2.1 nM.

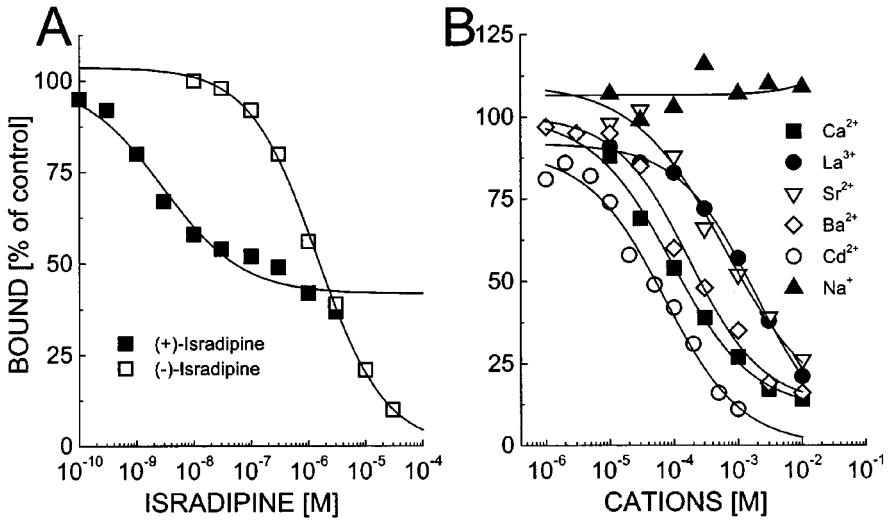

Figure 3 Modulation of [^{3}H]-mibefradil binding to skeletal muscle L-type Ca^{2+} channels by DHPs and cations. Membrane concentration was 8.8 μg ml^{-1}; radioligand concentration was 2.0 nM. (A) The following parameters were calculated by non-linear curve fitting: (+)-isradipine, IC_{50} = 1.6 nM, n_H = 0.94; inhibition to 42% of control; (−)-isradipine, IC_{50} = 1.4 μM, n_H = 0.77, complete inhibition. (B) Inhibition of [^{3}H]-mibefradil by cations: All cations were employed as chloride salts. The following binding parameters (IC_{50}, maximal inhibition) were obtained by linear curve fitting to the general-dose response equation: Cd^{2+}: 45 μM; 0% of control; Ba^{2+}: 310 μM; 12% of control; Ca^{2+}: 136 μM; 11% of control; La^{3+}: 1.3 mM; 0% of control; Sr^{2+}: 1.4 mM; 21% of control; Na^+: no inhibition. One of 2–3 similar experiments is shown.

Table 1 Modulation of [^{3}H]-mibfradil, (-)-[^{3}H]-devapamil and [^{3}H]-SQ32133 labelled L-type Ca^{2+} channels by mibefradil and its analogues

Compound	Stereo-chemistry	*[^{3}H]-Mibefradil*		*(−)-[^{3}H]-Devapamil skeletal muscle*		*[^{3}H]-SQ32,133*		*(−)-[^{3}H]-Devapamil brain*
		K_i (nM)	*Slope*	K_i (nM)	*Slope*	K_i (nM)	*Slope*	K_i (nM)
Mibefradil	1S,2S	1.2–1.5	0.79–0.86	1.67–1.8	0.98–1.06	2–2.1	1.09–1.23	2.6±0.7
RO-18-5881	1S,2S	0.26±0.03	0.92±0.03	0.36±0.03	1.15±0.09	0.45±0.04	1.42±0.07	0.20–0.30
RO-19-6945	racemic	1.1±0.2	1.18±0.1	1.8–2.6	1.44–1.46	n.d.	n.d.	2.9–3.3
RO-19-8287	racemic	2.0±0.34	1.26±0.1	3.5–4.2	1.1–1.16	n.d.	n.d.	3.0–4.2
RO-19-8531	1S,2S	3.3±0.7	0.86±0.06	2.2–3.7	0.89–1.02	2.3–2.4	0.91–1.19	n.d.
RO-19-9495	1R,2R	3.2±0.5	1.01±0.21	4.1–5.5	0.96–1.16	n.d.	n.d.	n.d.
RO-40-0293	1S,2S	2.8±0.4	1.07±0.15	2.8–3	0.91–1.05	4.6–5.9	1.47–1.66	3.1±0.3
RO-40-0713	1S,2S	1.3±0.09	0.83±0.08	1.6–2.1	0.95–1.2	1.6–1.7	1.02–1.24	n.d.
RO-40-6040	racemic	1.1±0.2	1.22±0.19	2.7±0.5	1.17±0.07	3.5±0.89	1.24±0.04	n.d.
RO-40-6088	1S,2S	5.4±0.4	1.01±0.11	11.8–14	1.66–1.83	12.9–14	1.90–2.07	2.3–4.7

K_i values were calculated according to Cheng & Prusoff, (1973) assuming a competitive interaction between radioligand and mibefradil. Data are expressed as means±s.e.mean for $n \geqslant 3$ or as range for $n=2$. n.d., not determined.

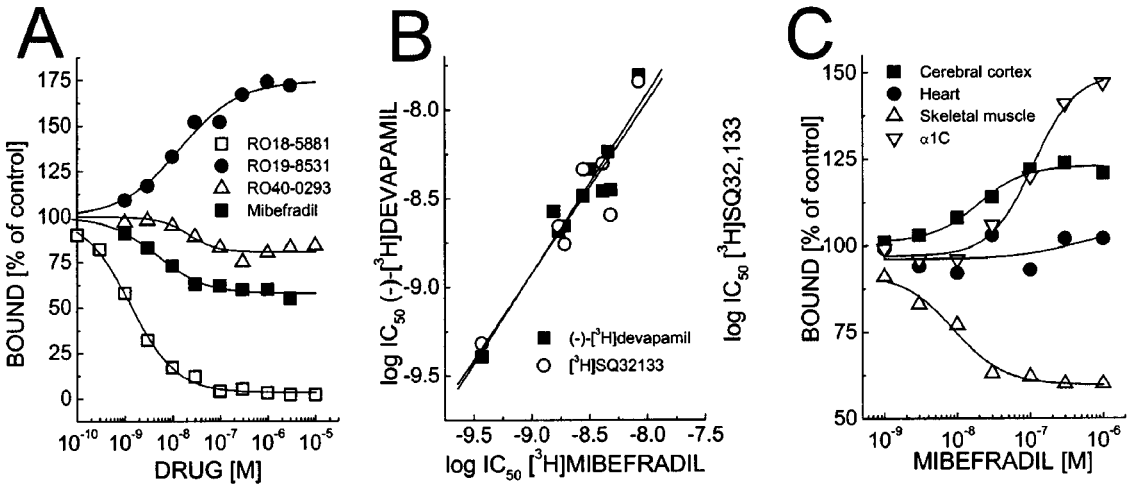

Figure 4 Modulation of drug binding to L-type Ca^{2+} channels by mibefradil and mibefradil analogues. (A) Modulation of (+)-[^{3}H]-isradipine binding to rabbit skeletal muscle Ca^{2+} channels. Radioligand concentration 0.3–1 nM; membrane protein concentration 8.8 μg ml^{-1}. The following binding parameters were determined by non-linear curve fitting (IC_{50} or EC_{50}; n_H; % maximal inhibition or stimulation: mibefradil: 4.2 nM, 0.94, 59% of control; RO18-5881: 1.34 nM, 0.91, 3% of control; RO19-8531: 14 nM, 0.7, 175% of control; RO40-0293: 22 nM 1.43, 81% of control. (B) Comparison of the apparent affinity of mibefradil and analogues for [^{3}H]-mibefradil, (−)-[^{3}H]-devapamil and [^{3}H]-SQ32133 labelled L-type Ca^{2+} channels. The IC_{50} values of mibefradil and its analogues for [^{3}H]-mibefradil labelled skeletal muscle Ca^{2+} channels are plotted against the corresponding IC_{50} values for (−)-[^{3}H]-devapamil ($r=0.95$, $n_H=1.01$) and [^{3}H]-SQ32133 ($r=0.92$, $n_H=0.97$) labelled channels, respectively. (C) Modulation of (+)-[^{3}H]-isradipine binding to L-type Ca^{2+} channels by mibefradil in cerebral cortex membranes (114 μg ml^{-1}), α1C/α2-δ/β1 expressing tsA201 cell membranes (60 μg ml^{-1}), rabbit heart membranes (82 μg ml^{-1}) and partially purified rabbit skeletal muscle transverse-tubule membranes (82 μg ml^{-1}). Radioligand concentration was 0.05–0.3 nM.

RO40-293, partial inhibition) indicating that this substituent sensitively effects the non-competitive interaction of mibefradil with the DHP binding domain. All other analogues were incomplete inhibitors of (+)-[^{3}H]-isradipine binding (not shown).

Mibefradil and its analogues completely inhibited (−)-[^{3}H]-devapamil and [^{3}H]-SQ32,133 binding with almost the same affinity as [^{3}H]-mibefradil-labeled channels and with Hill slopes close to unity (Table 1, Figure 4B). Taken together these data are consistent with a competitive interaction of mibefradil with the PAA and the BTZ binding domain.

High affinity of unlabelled mibefradil for neuronal L-type Ca^{2+} channels

Our finding that mibefradil inhibits DHP binding to skeletal muscle L-type Ca^{2+} channels (α1S subunit, Birnbaumer *et al*., 1994) is in contrast to the previously reported absence of DHP binding modulation in cardiac membranes (Rutledge & Triggle, 1995). Figure 4C illustrates that mibefradil indeed modulated DHP binding in a tissue-dependent manner. Whereas no concentration-dependent mibefradil effect was observed in rabbit heart membranes, the stimulatory effect on (+)-[^{3}H]-isradipine binding to brain L-type Ca^{2+} channels ($EC_{50}=15.2\pm5.6$ nM, $n=6$) and recombinant cardiac α1C subunits expressed in tsA201 cells ($EC_{50}=156\pm17$ nM, $n=5$) unmasked the high affinity of this drug for brain and cardiac L-type channels. Accordingly, mibefradil and its analogues also inhibited (−)-[^{3}H]-devapamil binding to guinea-pig brain membranes with IC_{50} values similar to those found in skeletal muscle (Table 1). Our data show that the non-competitive binding interaction between mibefradil and the DHP binding domain discriminates structural differences between α1 subunit isoforms (α1S in skeletal muscle vs α1C in heart and brain) and/or splice variants of α1C subunits in heart and brain (Snutch *et al*., 1991; Welling *et al*., 1997).

High affinity binding site for [^{3}H]-mibefradil in rabbit brain

To test if mibefradil also binds to neuronal Ca^{2+} channels other than L-type we performed direct labelling studies with [^{3}H]-mibefradil in rabbit brain membranes. A saturable binding component was detected which increased linearly with protein concentrations up to about 0.04 mg ml^{-1} (not shown). Scatchard transformation of the specific binding data revealed the existence of a single high affinity binding component ($K_D = 10.1 \pm 1.5$ nM, $B_{max} = 21.3 \pm 2.9$ pmol mg^{-1}) (Figure 5A, inset). Binding was not modulated by (+)- or (−)-isradipine ($n = 3$, not shown). Inhibition by (−)-devapamil (Figure 5A, see below) occurred with an IC_{50} two orders of magnitude higher than expected for L-type channels (Figure 2D, Goll *et al*., 1984a). Therefore L-type Ca^{2+} channels do not account for this binding component in accordance with their much lower density in mammalian brain (<1 pmol mg^{-1}, Striessnig *et al*., 1988).

To test the possible relationship of the [^{3}H]-mibefradil binding sites in brain membranes with non-L-type Ca^{2+} channels we tested the affinity of fluspirilene, pimozide and flunarizine which are blockers of non-L-type Ca^{2+} channels (Geer *et al*., 1993; Sah & Bean, 1993; Uneyama *et al*., 1997). All of them inhibited mibefradil binding with low nanomolar IC_{50} values (fluspirilene, $IC_{50} = 16.2 \pm 1.7$ nM, $n = 3$; pimozide, $IC_{50} = 19.6 \pm 4.6$ nM, $n = 3$; flunarizine, $IC_{50} = 32-36$ nM, range, $n = 2$) (Figure 5A). The IC_{50} of (−)-devapamil (215 ± 52 nM, $n = 3$) also agreed well the known 10–100 fold lower potency of PAAs for block of non-L-type as compared to L-type Ca^{2+} channels (Hockerman *et al*., 1997; Uneyama *et al*., 1997) in electrophysiological studies. Taken together these results do not rule out the possibility that [^{3}H]-mibefradil labels non-L-type ca^{2+} channels in mammalian brain but the lack of selectivity of these drugs for Ca^{2+} channels and their shallow inhibition curves prevented a pharmacological proof of this hypothesis.

We were unable to obtain other direct biochemical evidence for the interaction of [^{3}H]-mibefradil with non-L-type Ca^{2+} channels. After solubilization of prelabelled channels in digitonin for immunoprecipitation with anti-α1A (P/Q-type) and anti-β antibodies solubilized binding activity was too unstable for further analysis (not shown). We therefore expressed α1A subunits together with α2-δ and β subunits in tsA201 cells to directly measure binding of [^{3}H]-mibefradil to recombinant channels. A high affinity binding site for [^{3}H]-mibefradil was present at similar densities in membrane preparations of both α1A/α2-δ/β but also of mock transfected cells ($K_D = 1.02 \pm 0.16$ nM, $B_{max} = 1.08 \pm 0.37$ pmol mg^{-1} of protein, $n = 4$). This endogenous site was not characterized further but prevented sensitive detection of [^{3}H]-mibefradil interaction with expressed Ca^{2+} channels in tsA201 and HEK 293 cells. It seemed not to be associated with metabolic enzymes as it was absent in liver membrane preparations (not shown).

Since flunarizine also blocks neuronal voltage-gated Na^+-channels (Kiskin *et al*., 1993) and the Na^+-channel blocker DPI201-106 displayed also high affinity ($IC_{50} = 28 \pm 2.9$ nM, $n = 3$; Figure 5A) for the [^{3}H]-mibefradil labelled sites, we tested the possibility that at least part of the [^{3}H]-mibefradil binding occurs to voltage-gated Na^+-channels. To this end we labelled brain Na^+-channels with the high affinity Na^+-channel-selective probe [^{3}H]-WIN17317-3 (Wanner *et al*., 1999). Its binding properties in guinea-pig synaptic plasma membranes were consistent with high affinity labelling of voltage-gated Na^+-channels ($K_D = 4.4 \pm 1.0$ nM, $B_{max} = 10.0 \pm 2.9$ pmol mg^{-1} of protein, $n = 3$; Figure 5B). The typical binding stimulation by 1 μM phenytoin was also observed ($n = 2$; Wanner *et al*., 1999). Mibefradil ($K_i = 17.2 \pm 1.8$ nM, $n = 3$) as well as its analogues completely inhibited [^{3}H]-WIN17317-3 binding with low nanomolar IC_{50} values (Figure 5B; Table 2). The affinity of the mibefradil analogues for [^{3}H]-WIN17317-3-labelled Na^+-channels did not correlate with their affinity for skeletal muscle Ca^{2+} channels (Table 2) suggesting that binding to Na^+-channels occurs with a different structure-activity relationship.

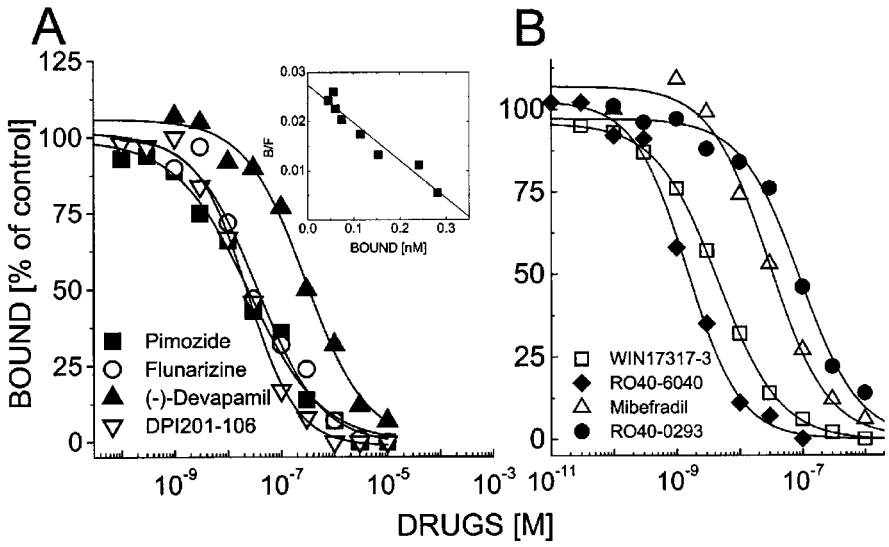

Figure 5 [^{3}H]-mibefradil and [^{3}H]-WIN17317-3 binding to cerebral cortex membranes. (A) Inhibition of [^{3}H]-mibefradil binding to rabbit cerebral cortex membranes. The following binding parameters were determined by nonlinear curve-fitting (IC_{50}; n_H): pimozide: 25 nM, 0.64; flunarizine: 33 nM, 0.73; devapamil: 310 nM; 0.86; DPI 201–106: 23 nM, 0.93. Radioligand and membrane protein concentrations were 1–1.9 nM and 14–21 μg ml^{-1}, respectively. Inset: Saturation analysis of [^{3}H]-mibefradil binding to cerebral cortex membranes: r = 0.96; $K_D = 8.4$. nM, $B_{max} = 17$ pmol mg^{-1} of protein. (B) Inhibition of [^{3}H]-WIN17317-3 binding to guinea-pig synaptic plasma membranes. The following binding parameters were determined by nonlinear curve fitting (IC_{50}; n_H): WIN17317-3: 4.6 nM, 0.89; mibefradil: 29 nM, 0.93; RO40-0293: 92 nM, 0.92; RO40-6040: 15 nM, 1.04. Radioligand and membrane protein concentrations were 1.4–1.8 nM and 26 μg ml^{-1}, respectively.

This was especially evident for compound RO18-5881, which has 127 fold lower affinity for Na^+- than for Ca^{2+} channels (Table 2).

To prove the Na^+-channel activity of mibefradil in functional experiments the effect of increasing concentrations of mibefradil on Na^+-currents in GH3 cells was measured using the whole-cell patch clamp technique. Na^+-inward current (I_{Na}) was elicited by 5 ms depolarizations from a holding potential of −80 mV to +5 mV at a frequency of 3 Hz. The concentration-dependent tonic (measured as block of I_{Na} during the first pulse after incubation with the drug) and use-dependent block (observed at the end of the pulse train) are shown in Figure 6A,B. Under these experimental conditions half-maximal use-dependent block occurred around 1 μM. This concentration is similar to those reported for half-maximal block of native (Liu *et al*., 1999; Mishra & Hermsmeyer, 1994) and recombinant (Bezprozvanny & Tsien, 1995; Cribbs *et al*., 1998; Mehrke *et al*., 1994; Williams *et al*., 1999) T- and L-type Ca^{2+} channels in muscle cells.

To evaluate if use-dependent inhibition (Figure 6) reflects preferential block of open or inactivated Na^+ channels we increased the time which the channel spends in the inactivated state by increasing the duration of individual pulses during the train from 5 to 50 ms. Neither the extent (Figure 6C) nor the time course of block development (Figure 6D) were changed during 50 ms pulse trains arguing against a role of inactivation for mibefradil action.

Table 2 Inhibition of [^{3}H]-WIN17317-3 binding to voltage-gated Na^+ channels by mibefradil and its analogues

Drug	K_i (nM)	n_H	*Ratio*
Mibefradil	17±1.8	0.98±0.05	12.6
RO18-5881	33±4.6	0.89±0.14	127
RO19-6945	2.4±0.5	0.79±0.08	2.2
RO19-8287	8.4±0.6	0.97±0.10	4.2
RO19-8531	32±3.2	0.89±0.08	9.7
RO19-9495	8.1±1.6	0.83±0.02	2.5
RO40-0293	51±13	0.97±0.03	18
RO40-0713	20±4.2	0.82±0.11	15
RO40-6040	1.0±0.3	1.15±0.06	0.9
RO40-6088	2.8±0.6	0.82±0.02	0.5

K_i values were calculated according to Cheng & Prusoff (1973) assuming competitive inhibition. The ratio of the binding affinities for [^{3}H]-WIN17317-3 labelled Na^+ channels vs [^{3}H]-mibefradil labelled Ca^+ channels (data taken from Table 1) are given. Means±s.e.mean for $n>3$.

Discussion

Our experiments show that mibefradil interacts with skeletal muscle and brain L-type Ca^{2+} channels with high affinity. In skeletal muscle its binding properties are compatible with competitive interaction at the PAA/BTZ binding domain as

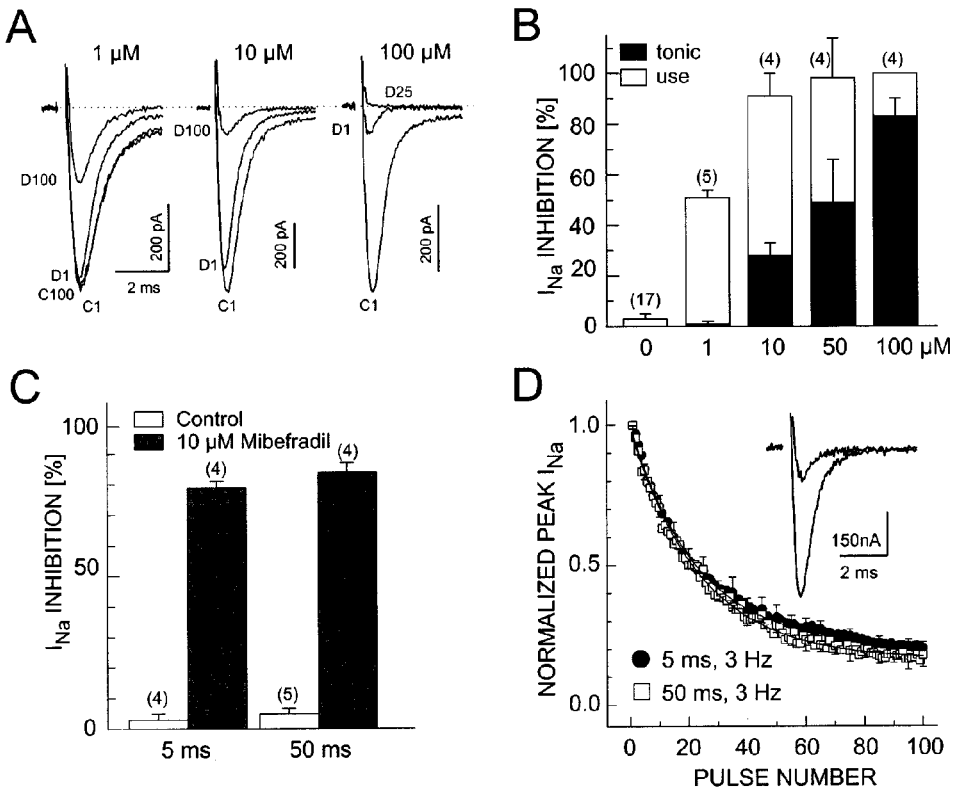

Figure 6 Inhibition of I_{Na} by mibefradil in GH3 cells. (A) Inward currents through voltage-dependent Na^+-channels were elicited by 3 Hz trains of 5 ms depolarizations from a holding potential of −80 mV to +5 mV before and after incubation of the cell in 1 (left), 10 μM (middle) and 100 μM (right) mibefradil. The first, 25th and/or 100th pulse of the train in the absence (C1, C100) and presence (D1, D25, D100) of drug are indicated. (B) Tonic (black) and use-dependent (white) block induced by increasing concentrations of mibefradil during a train of 100 test pulses (5 ms, 3 Hz) are shown as means±s.e.mean for the indicated number of experiments. (C) Use-dependent I_{Na} inhibition during a train of 100 test pulses (5 or 50 ms) in the absence (white) or presence of 10 μM mibefradil (black). Data are shown as means±s.e.mean for the indicated number of experiments. (D) Use-dependent I_{Na} inhibition during 3 Hz-pulse trains from −80 to 5 mV of 5 or 50 ms test pulses. The kinetics of use-dependent block were fitted to single exponential functions with corresponding time constants of peak I_{Na} decay of 7.4±0.7 and 7.9±0.7 ms ($n=4$, $P>0.05$). Data are shown as means±s.e.mean for $n=4$. Inset: Representative I_{Na} (10 μM mibefradil present) during the first and 100th 50 ms-pulse of a 3 Hz-pulse train.

implicated by the following properties: like for the PAA [^{3}H]-verapamil (Goll *et al*., 1984b) its binding density was higher than for DHPs, [^{3}H]-mibefradil binding was inhibited by unlabelled PAAs in an apparently competitive manner; a series of mibefradil analogues blocked (−)-[^{3}H]-devapamil and [^{3}H]-SQ32,133 interaction with IC_{50} values corresponding to their affinity for the [^{3}H]-mibefradil-labelled channel. In addition, the dissociation rate increased as a function of unlabelled ligand concentration as previously described for PAAs (Goll *et al*., 1984b) and BTZs (Prinz & Striessnig, 1993). This 'ligand-induced accelerated dissociation' indicates that more than one mibefradil molecule can bind to the channel at the same time (Prinz & Striessnig, 1993). Like PAAs and BTZs, mibefradil and its derivatives non-competitively inhibit or stimulate DHP binding (Glossmann *et al*., 1985). Taken together these results strongly indicate that mibefradil binds to the same multisubsite domain on the α1 subunit of L-type Ca^{2+} channels that contains the closely associated interaction sites for DHPs, PAAs and BTZs (Hockerman *et al*., 1997; Striessnig *et al*., 1998). This is further supported by our recent finding that mibefradil not only stimulates DHP binding to recombinant α1C and brain L-type channels (this study) but also to a recombinant DHP binding domain transferred into previously DHP insensitive α1A subunits by site-directed mutagenesis (Huber *et al*., 2000).

We further demonstrate that mibefradil and some of its analogues display high affinity for neuronal voltage-gated Na^+-channels. Like [^{3}H]-WIN17317-3 (Wanner *et al*., 1999) mibefradil must be selective for neuronal vs cardiac Na^+-channels because of the reported weak Na^+-channel blocking activity in mammalian heart (Hoffmann-La Roche Inc., 1994). Enhanced inactivation did not affect use-dependent Na^+ channel block of GH3 cells (Figure 6C,D). This result is in line with previous reports of Aczél *et al*. (1998) on mibefradil block of P/Q-type Ca^{2+} channels and suggests an open state- but not inactivated state-dependent block mechanism in both channel types.

The potential of mibefradil to block both neuronal Na^+-channels as well as a wide spectrum of voltage-gated Ca^{2+} channels is of high pharmacological interest. Block of Na^+- (e.g. phenytoin, carbamazepine, lamotrigine) as well as T-type Ca^{2+} channels (e.g. phenytoin, ethosuximide) is believed to cause antiepileptic effects (MacDonald & Kelly, 1995; Todorovic & Lingle, 1998). Likewise, block of Na^+-channels (e.g. riluzole, lifarizine; Bryson *et al*., 1996; McGivern *et al*., 1995) as well as N-type Ca^{2+} channels (SNX-111; Miljanich & Ramachandran, 1995) results in neuroprotective effects. Therefore lipophilic mibefradil derivatives with high brain penetration may represent interesting anticonvulsant as well as neuroprotective drugs.

Mibefradil has recently been shown to block L- and non-L-type Ca^{2+} channels, including low voltage activated T-type channels, expressed in *Xenopus* oocytes with similar affinity (Bezprozvanny & Tsien, 1995). This suggests that high affinity binding domains should also be located on non-L-type Ca^{2+} channel α1 subunits such as α1A (P/Q-type), α1B (N-type) and α1E (R-type). Although we demonstrated the existence of high affinity binding sites ($K_D = 10$ nM, $B_{max} = 21$ pmol mg^{-1}) for [^{3}H]-mibefradil in mammalian brain we were unable to prove their association with non-L-type Ca^{2+} channels. It is difficult to relate the B_{max} of the [^{3}H]-mibefradil labelled sites to the density of all cloned Ca^{2+} channel types taken together. L-type (0.5–0.9 pmol mg^{-1} of (+)-[^{3}H]-isradipine or (−)-[^{3}H]-devapamil binding; Striessnig *et al*., 1988), P/Q-type (up to 3 pmol mg^{-1} of [^{125}I]-omega-conotoxin MVIIC binding; Pichler *et al*., 1996) and N-type (up to 1 pmol mg^{-1} of [^{125}I]-omega-conotoxin GVIA binding; Knaus *et al*., 1987) channels account for about 5 pmol of sites per mg of protein. However, due to the lack of specific radioligands the density of R-type (α1E) and T-type channels (α1G, α1I), which together with Na^+-channels may also contribute to [^{3}H]-mibefradil binding in brain, is still unknown.

The presence of a high affinity binding site in tsA201 cells was unexpected and prevented the further analysis of [^{3}H]-mibefradil interaction with recombinant non-L-type Ca^{2+} channel α1 subunits. As for [^{3}H]-mibefradil binding in brain we lack specific pharmacological tools to prove if these sites are associated with the endogenous Ca^{2+} channels previously identified in HEK 293 cells (Berjukow *et al*., 1996).

Taken together our data demonstrate that structural modification of mibefradil results in compounds with even higher affinity for Na^+- (e.g. RO40-6040) or Ca^{2+} channels (e.g. RO18-5881) than mibefradil itself. Thus our study emphasizes the need to screen mibefradil analogues for compounds with higher affinity for non-L-type Ca^{2+} channels which could help to develop the first generation of non-peptide radioligands for non-L-type Ca^{2+} channels. Such ligand would provide us with radioligand-based screening assays to develop non-L-type Ca^{2+} channel-active compounds. Such compounds are believed to represent important therapeutics for the treatment of severe pain (Miljanich & Ramachandran, 1995), migraine (Kraus *et al*., 1998a) and cerebral ischaemia (Miljanich & Ramachandran, 1995).

We thank D. Ostler for expert technical assistance and Dr Thierry Langer for critical comments on the manuscript. This work was supported by the Fonds zur Förderung der Wissenschaftlichen Forschung (FWF grants P12641 to J. Striessnig, P12649 to S. Hering), the Österreichische Nationalbank (6573 to J. Striessnig) and the Dr Legerlotz Foundation.

References

ACZEL, S., KURKA, B. & HERING, S. (1998). Mechanism of voltage- and use-dependent block of class A Ca^{2+} channels by mibefradil. *Br. J. Pharmacol.,* **125,** 447–454.

BERJUKOW, S., DÖRING, F., FROSCHMAYR, M., GRABNER, M., GLOSSMANN, H. & HERING, S. (1996). Endogenous calcium channels in human embryonic kidney (HEK293) cells. *Br. J. Pharmacol.,* **118,** 748–754.

BEZPROZVANNY, I. & TSIEN, R.W. (1995). Voltage-dependent blockade of diverse types of voltage-gated Ca^{2+} channels expressed in Xenopus oocytes by the Ca^{2+} channel antagonist mibefradil (Ro 40-5967). *Mol. Pharmacol.,* **48,** 540–549.

BIRNBAUMER, L., CAMPBELL, K.P., CATTERALL, W.A., HARPOLD, M.M., HOFMANN, F., HORNE, W.A., MORI, Y., SCHWARTZ, A., SNUTCH, T.P., TANABE, T. & TSIEN, R.W. (1994). The naming of voltage-gated calcium channels. *Neuron,* **13,** 505–506.

BRYSON, H.M., FULTON, B. & BENFIELD, P. (1996). Riluzole. A review of its pharmacodynamic and pharmacokinetic properties and therapeutic potential in amyotrophic lateral sclerosis. *Drugs,* **52,** 549–563.

CHENG, Y. & PRUSOFF, W.H. (1973). Relationship between the inhibition constant (Ki) and the concentration of inhibitor which causes 50 per cent inhibition (IC50) of an enzymatic reaction. *Biochem. Pharmacol.,* **22,** 3099–3108.

CLOZEL, J.P., ERTEL, E.A. & ERTEL, S.I. (1997). Discovery and main pharmacological properties of mibefradil (Ro 40-5967), the first selective T-type calcium channel blocker. *J. Hypertens.* **15** (Suppl.): S17–S25.

CRIBBS, L.L., LEE, J.H., YANG, J., SATIN, J., ZHANG, Y., DAUD, A., BARCLAY, J., WILLIAMSON, M.P., FOX, M., REES, M. & PEREZ-REYES, E. (1998). Cloning and characterization of alpha1H from human heart, a member of the T-type Ca^{2+} channel gene family. *Circ. Res.,* **83,** 103 – 109.

FEIGENBAUM, P., GARCIA, M.L. & KACZOROWSKI, G.J. (1988). Evidence for distinct sites coupled to high affinity omega-conotoxin receptors in rat brain synaptic plasma membrane vesicles. *Biochem. Biophys. Res. Commun.,* **154,** 298 – 305.

GEER, J.J., DOOLEY, D.J. & ADAMS, M.E. (1993). K(+)-stimulated $^{45}Ca^{2+}$ flux into rat neocortical mini-slices is blocked by omega-Aga-IVA and the dual Na^+/Ca^{2+} channel blockers lidoflazine and flunarizine. *Neurosci. Lett.,* **158,** 97 – 100.

GLOSSMANN, H. & FERRY, D.R. (1985). Assay for calcium channels. *Meth. Enzymol.,* **109,** 513 – 550.

GLOSSMANN, H., FERRY, D.R., GOLL, A., STRIESSNIG, J. & ZERNIG, G. (1985). Calcium channels and calcium channel drugs: recent biochemical and biophysical findings. *Drug Res.,* **35,** 1917 – 1935.

GLOSSMANN, H., LINN, T., ROMBUSCH, M. & FERRY, D.R. (1983). Temperature-dependent regulation of d-cis [^{3}H]-diltiazem binding to Ca^{2+} channels by 1.4-dihydropyridine channel agonists and antagonists. *FEBS Lett.,* **160,** 226 – 232.

GOLL, A., FERRY, D.R. & GLOSSMANN, H. (1984b). Target size analysis and molecular properties of Ca2+ channels labelled with [^{3}H] verapamil. *Eur. J. Biochem.,* **141,** 177 – 186.

GOLL, A., FERRY, D.R., STRIESSNIG, J., SCHOBER, M. & GLOSSMANN, H. (1984a). (−)-[^{3}H] desmethoxyverapamil, a novel Ca^{2+} channel probe: binding characteristics and target size analysis of its receptor in skeletal muscle. *FEBS Lett.,* **176,** 371 – 377.

HAMILL, O.P., MARTY, A., NEHER, E., SAKMANN, B. & SIGWORTH, F.J. (1981). Improved patch-clamp techniques for high-resolution recording from cell and cell-free membrane patches. *Pflügers Arch.,* **391,** 85 – 100.

HERING, S., SAVCHENKO, A., STRÜBING, C., LAKITSCH, M. & STRIESSNIG, J. (1993). Extracellular localization of the benzothiazepine binding domain of L-type calcium channels. *Mol. Pharmacol.,* **43,** 820 – 826.

HOCKERMAN, G.H., JOHNSON, B.D., ABBOTT, M.R., SCHEUER, T. & CATTERALL, W.A. (1997). Molecular determinants of high affinity phenylalkylamine block of L-type calcium channels in transmembrane segment IIIS6 and the pore region of the alpha1 subunit. *J. Biol. Chem.,* **272,** 18759 – 18765.

HOFFMANN-LA ROCHE INC. (1994). RO40-5967 (Mibefradil). *Investigational Drug Brochure*.

HUBER, I., WAPPL, E., HERZOG, A., MITTERDORFER, J., GLOSSMANN, H., LANGER, T. & STRIESSNIG, J. (2000). Conserved Ca^{2+} antagonist binding properties and putative folding structure of a recombinant high affinity dihydropyridine binding domain. *Biochem. J.,* in press.

KISKIN, N.I., CHIZHMAKOV, I.V., TSYNDRENKO, A.Y., KRISHTAL, O.A. & TEGTMEIER, F. (1993). R56865 and flunarizine as Na^+-channel blockers in isolated Purkinje neurons of rat cerebellum. *Neuroscience,* **54,** 575 – 585.

KNAUS, H.G., STRIESSNIG, J., KOZA, A. & GLOSSMANN, H. (1987). Neurotoxic aminoglycoside antibiotics are potent inhibitors of [^{125}I]-omega-conotoxin GVIA binding to guinea-pig cerebral cortex membranes. *Naunyn-Schmiedeberg's Arch. Pharmacol.,* **336,** 583 – 586.

KRAUS, R.L., HERING, S., GRABNER, M., OSTLER, D. & STRIESSNIG, J. (1998b). Molecular mechanism of diltiazem interaction with L-type calcium channels. *J. Biol. Chem.,* **273,** 27205 – 27212.

KRAUS, R.L., SINNEGGER, M.J., GLOSSMANN, H., HERING, S. & STRIESSNIG, J. (1998a). Familial hemiplegic migraine mutations change alpha1A calcium channel kinetics. *J. Biol. Chem.,* **273,** 5586 – 5590.

LIU, J.H., BIJLENGA, P., OCCHIODORO, T., FISCHER-LOUGHEED, J., BADER, C.R. & BERNHEIM, L. (1999). Mibefradil (Ro 40-5967) inhibits several Ca^{2+} and K^+ currents in human fusion-competent myoblasts. *Brit. J. Pharmacol.,* **126,** 245 – 250.

LOWRY, O.H., ROSEBROUGH, N.H., FARR, A.L. & RANDALL, F.J. (1951). Protein measurement with the Folin reagent. *J. Biol. Chem.,* **193,** 265 – 275.

MACDONALD, R.L. & KELLY, K.M. (1995). Antiepileptic drug mechanisms of action. *Epilepsia,* **36** (Suppl 2): S2 – S12.

MCGIVERN, J.G., PATMORE, L. & SHERIDAN, R.D. (1995). Actions of the novel neuroprotective agent, lifarizine (RS-87476), on voltage-dependent sodium currents in the neuroblastoma cell line, N1E-115. *Br. J. Pharmacol.,* **114,** 1738 – 1744.

MEHRKE, G., ZONG, X.G., FLOCKERZI, V. & HOFMANN, F. (1994). The Ca^{2+}-channel blocker Ro 40-5967 blocks differently T-type and L-type Ca^{2+} channels. *J. Pharmacol. Exp. Ther.,* **271,** 1483 – 1488.

MILJANICH, G.P. & RAMACHANDRAN, J. (1995). Antagonists of neuronal calcium channels: Structure, function and therapeutic implications. *Annu. Rev. Pharmacol. Toxicol.,* **35,** 707 – 734.

MISHRA, S.K. & HERMSMEYER, K. (1994). Selective inhibition of T-type Ca^{2+} channels by Ro 40-5967. *Circ. Res.,* **75,** 144 – 148.

MITTERDORFER, J., SINNEGGER, M.J., GRABNER, M., STRIESSNIG, J. & GLOSSMANN, H. (1995). Coordination of Ca2+ by the pore region glutamates is essential for high-affinity dihydropyridine binding to the cardiac Ca^{2+} channel alpha1 subunit. *Biochemistry,* **34,** 9350 – 9355.

OSTERRIEDER, W. & HOLCK, M. (1989). In vitro pharmacologic profile of Ro 40-5967, a novel calcium channel blocker with potent vasodilator but weak inotropic action. *J. Cardiovasc. Pharmacol.,* **13,** 754 – 759.

PICHLER, M., WANG, Z., GRABNER-WEISS, C., REIMER, D., HERING, S., GRABNER, M., GLOSSMANN, H. & STRIESSNIG, J. (1996). Block of P/Q-type calcium channels by therapeutic concentrations of aminoglycoside antibiotics. *Biochemistry,* **35,** 14659 – 14664.

PRINZ, H. & STRIESSNIG, J. (1993). Ligand-induced accelerated dissociation of (+)-cis-diltiazem from L-type calcium-channels is simply explained by competition for individual attachment points. *J. Biol. Chem.,* **268,** 18580 – 18585.

RATNER, E.I., BOCHKOV, V.N. & TKACHUK, V.A. (1996). Comparison of binding of [^{3}H] desmethoxyverapamil and 3H-mibefradil in vascular smooth muscle and heart membranes. Possible binding of mibefradil to a site distinct from the phenylalkylamine-binding site. *Arzneimittelforschung,* **46,** 953 – 955.

RUTLEDGE, A. & TRIGGLE, D.J. (1995). The binding interactions of Ro 40-5967 at the L-type calcium channel in cardiac tissue. *Eur. J. Pharmacol.,* **280,** 155 – 158.

SAH, D.W.Y. & BEAN, B.P. (1993). Inhibition of P-type and N-type calcium channels by dopamine receptor antagonists. *Mol. Pharmacol.,* **45,** 84 – 92.

SNUTCH, T.P., TOMLINSON, W.J., LEONARD, J.P. & GILBERT, M.M. (1991). Distinct calcium channels are generated by alternative splicing and are differentially expressed in the mammalian CNS. *Neuron,* **7,** 45 – 57.

STRIESSNIG, J., GRABNER, M., MITTERDORFER, J., HERING, S., SINNEGGER, M.J. & GLOSSMANN, H. (1998). Structural basis of drug binding to L calcium channels. *Trends Pharmacol. Sci.,* **19,** 108 – 115.

STRIESSNIG, J., KNAUS, H.G. & GLOSSMANN, H. (1988). Photoaffinity-labelling of the calcium-channel-associated 1,4-dihydropyridine and phenylalkylamine receptor in guinea-pig hippocampus. *Biochem. J.,* **253,** 39 – 47.

TODOROVIC, S.M. & LINGLE, C.J. (1998). Pharmacological properties of T-type Ca^{2+} current in adult rat sensory neurons: effects of anticonvulsant and anesthetic agents. *J. Neurophysiol.,* **79,** 240 – 252.

UNEYAMA, H., TAKAHARA, A., DOHMOTO, H., YOSHIMOTO, R., INOUE, K. & AKAIKE, N. (1997). Blockade of N-type Ca^{2+} current by cilnidipine (FRC-8653) in acutely dissociated rat sympathetic neurones. *Brit. J. Pharmacol.,* **122,** 37 – 42.

WANNER, S.G., GLOSSMANN, H., KNAUS, H.G., BAKER, R., PARSONS, W., RUPPRECHT, K., BROCHU, R., COHEN, C.J., SCHMALHOFER, W.A., SMITH, M.M., WARREN, W., GARCIA, M.L. & KACZOROWSKI, G.J. (1999). WIN 17317-3, a high-affinity probe for voltage-gated Na+ channels. *Biochemistry,* **38,** 11137 – 11146.

WELLING, A., LUDWIG, A., ZIMMER, S., KLUGBAUER, N., FLOCKERZI, V. & HOFMANN, F. (1997). Alternatively spliced IS6 segments of the alpha 1C gene determine the tissue-specific dihydropyridine sensitivity of cardiac and vascular smooth muscle L-type Ca^{2+} channels. *Circ. Res.,* **81,** 526 – 532.

WILLIAMS, M.E., WASHBURN, M.S., HANS, M., URRUTIA, A., BRUST, P.F., PRODANOVICH, P., HARPOLD, M.M. & STAUDERMAN, K.A. (1999). Structure and functional characterization of a novel human low-voltage activated calcium channel. *J. Neurochem.,* **72,** 791 – 799.

(Received November 29, 1999
Revised February 24, 2000
Accepted March 8, 2000)